Use-dependent reorganization of spared and severed descending pathways after contusion SCI in rats

Master student: Audrey Nguyen, UNIL

Director: Prof. Grégoire Courtine, EPFL

Supervisor: Janine Beauparlant, EPFL

Expert: Dr. Jocelyne Bloch, CHUV-UNIL

Lausanne, June 2014

Table of contents

Abbreviations

AAV1: Adeno-associated virus, serotype 1

BDA: Biotinylated dextran amine

CMV: Cytomegalovirus

CST: Corticospinal tract

EES: Epidural electrical stimulation

FB: Fastblue

GFP: Green fluorescent protein

i.p.: Intraperitoneal

ReST: Reticulospinal tract

SCI: Spinal cord injury

Abstract

Most spinal cord injuries (SCIs) in humans result from a blunt trauma to the spine leading to contusion of the spinal cord and half of these accidents lead to chronic paralysis below the level of injury. However, even in those paralyzed patients, histological analyses reveal a subset of spared descending fibers in the majority of cases (Kakulas, 1999; Norenberg *et al.*, 2004). Severe contusion SCI in rats reproduces these anatomical and functional features. We assessed the effects of neuroprosthetic rehabilitation on recovery of voluntary locomotion using this model.

Neuroprosthetic rehabilitation was recently introduced and tested on rats staggered hemisection SCI that interrupted all direct descending projections while leaving a gap of interconnected intact neural tissue. The therapy demonstrated unprecedented functional results with electrochemically-enabled restoration of voluntary movements, including walking, running and stair-climbing (van den Brand *et al.*, 2012). In the case of contused SCI rats, neuroprosthetic rehabilitation led to an enhanced functional outcome including the ability to sustain voluntary walking in the absence of any enabling factor in half of the trained animals.

In the present project, we aimed at characterizing the changes in corticospinal and reticulospinal pathways in trained rats that regained supraspinal control over their hindlimbs following neuroprosthetic rehabilitation and in non-trained rats. We show that the spared reticulospinal tract (ReST) underwent reorganization in response to neuroprosthetic rehabilitation below but not above the lesion level. Additionally, we found extensive spontaneous sprouting of the corticospinal tract (CST) above the lesion. These results, together with significant secondary damages and neuroprotection, highlight the mechanisms that are specifically related to recovery of voluntary locomotion in our clinically relevant contusion model.

Key words: contusion, corticospinal tract, reticulospinal tract, neuroprosthetic rehabilitation, spinal cord injury, sprouting

Introduction

Spinal cord injury (SCI) occurs with an incidence rate ranging between 12 and 58 per million inhabitants per year worldwide (van den Berg *et al.*, 2010) and is therefore a major concern for public health. Mechanical traumatisms account for the majority of SCI, with a peak of incidence in the 18-32 years old population (Lee *et al.*, 2014). Thus the impact in terms of years lived with disability is high, since half of SCI result in permanent paralysis. Quality of life is compromised as well in SCI patients, due to bladder, bowel and sexual dysfunctions, chronic pain, increased susceptibility to infections and to other medical conditions.

However, even in a complete cord syndrome, defined as a complete loss of motor and sensory functions below the level of injury ("ASIA A" in the American Spinal Injury Association scaling), in most cases a subset of descending fibers is spared (1-10%) at the injury level (Kakulas, 1999; Norenberg *et al.*, 2004). Such a remaining bridge was first evidenced *in vivo* by Dimitrijevic and colleagues (Dimitrijevic *et al.*, 1983) who measured a residual electrophysiological conductance across the lesion in human subjects with a clinically complete SCI. Over the past decades, lot of effort has been put based on the conception that this anatomical substrate could be a promising candidate to re-establish top-down long-distance connections for motor control recovery. These attempts were based on modifying the microenvironment of the lesion to enhance spontaneous sprouting of the spared fibers. Strategies have included molecules that inhibit the reactive deleterious factors secreted by the tissue: for example treatments with chondroitinase (Bradbury *et al.*, 2002), and anti-NogoA antibodies (Schnell & Schwab, 1990). In parallel, there has also been research in the field of axonal regeneration, including re-expression of Wnt gradients (Hollis ER *et al.*, 2012) and growth factors enrichment. But the adult CNS has demonstrated very limited capacities to regrow an axon once it has been injured. So far, results are modest, especially when it comes to translational and clinical experiments. The complexity of the lesion environment constitutes a considerable challenge that would be likely difficult to overcome with a single molecular target.

Unprecedented functional results in a rat model with restoration of near-physiological gait patterns, were achieved when capitalizing on the power of lumbosacral circuits using a more generalized approach, i.e. in combination with physical activity (Courtine *et al.*, 2009). Following the lesion, lumbosacral circuits are disconnected from supraspinal control and thus can be considered being in a dormant state. Using an electrochemical neuroprosthesis (Musienko *et al.*, 2009; Musienko *et al.*, 2011), they can be transformed into a highly functional state: monoaminergic agonists raise the level of neuronal excitability while continuous epidural stimulation engages spinal circuits which in turn

facilitates locomotion. However, due to the complete and permanent interruption of supraspinal input, stepping on the treadmill remained automatic and involuntary.

In cases where there was some intraspinal continuity left at the level of the lesion, there was a hypothesis for additionally recovering a supraspinal control over these lumbosacral circuits. A robotic postural interface was hence designed to encourage voluntary stepping (Dominici *et al.*, 2012).

"Neuroprosthetic rehabilitation" (also called "multi-system neurorehabilitation") composed of electrochemical stimulation together with the use of robotic postural interface in a context of positive reinforcement was tested on rats with midthoracic staggered lateral hemisection SCI. In this model, all direct descending projections were interrupted while leaving a gap of spared interconnected tissue. Functional results were impressive with rats that regained the ability of full-weight bearing voluntary walking, swimming and stair climbing in the presence of the electrochemical stimulation. Anatomical examination revealed extensive and ubiquitous remodeling of cortical projections and spared neuronal circuitries (van den Brand *et al.*, 2012).

This "proof of concept" opened a way towards investing in a new therapy for patients with SCI, however there was still some unanswered questions. The next milestone to reach was to assess the effect of a similar training strategy in a clinically more relevant model. Indeed, cut injuries are rather rare in human SCI. Instead, SCI are often the result of a mechanical trauma that creates a primary lesion called "contusion". As opposed to a cut injury, the contusion brings a series of prominent secondary damage including the formation of cavities, glial scar, demyelination of surrounding fibers, Wallerian degeneration and the secretion of an array of inhibitory molecules (Norenberg *et al.*, 2004). Together, they compromise the chances of the CNS to undergo constructive plasticity. Weight-drop contusion SCI in rats is a model that has similar functional, electrophysiological and morphological outcomes compared to human SCI (Metz *et al.*, 2000). It was therefore used as a model of severe contusion SCI in a paradigm of neuroprosthetic rehabilitation.

After 9 weeks of training, all rats had regained coordinated overground locomotion when supplied with electrochemical stimulation. More strikingly, half of them were able to sustain voluntary walking in the complete absence of stimulation (**Figure 1** D), a result of great importance when considering the translation to human therapeutics.
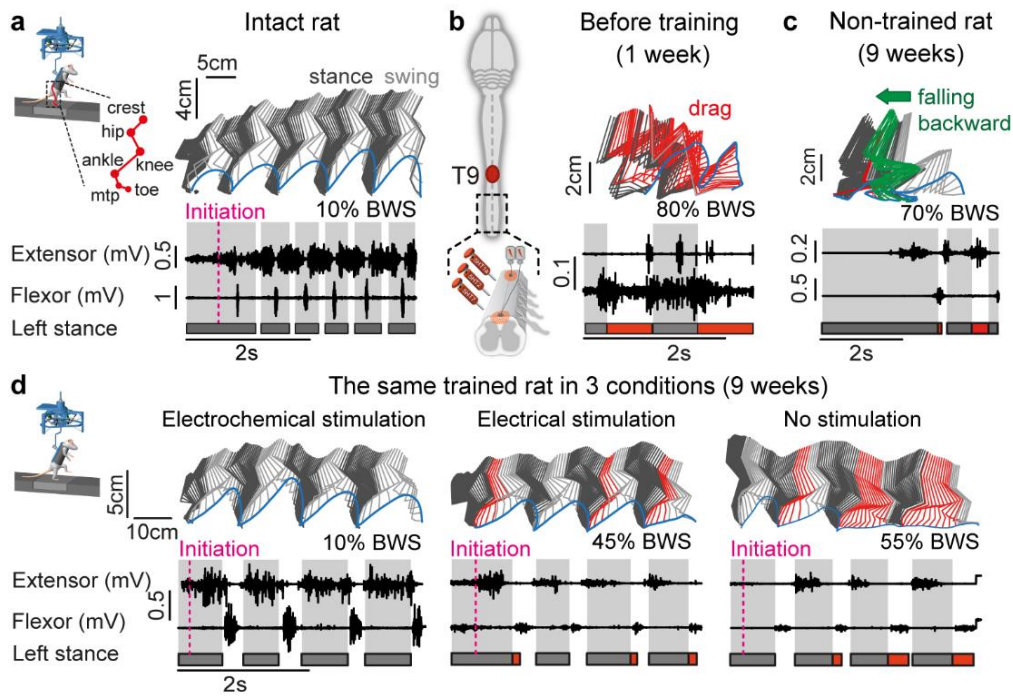
Figure 1. Functional results of neuroprosthetic rehabilitation applied to rats with severe contusion SCI. Recordings from a healthy rat (A), lesioned rat before training (B), non-trained rat after 9 weeks (C) and trained rat after 9 weeks (D). Each panel shows the endpoint (mtp joint) trajectory of the rat's hindlimb (blue line) together with EMG activity in extensor (medial gastrocnemius) and flexor (tibialis anterior) muscles. BWS, body-weight support; mtp, metatarsophalangeal.

Aim of this project

Which are the mechanisms underlying the functional response to neuroprosthetic rehabilitation in the contusion SCI model? To address this question, we have focused in this project on the neuroanatomical examination of the spinal cord segments above and below the lesion. We aimed at characterizing the reorganization of spared and severed descending fibers of both corticospinal and reticulospinal pathways.

We hypothesized that i) severed corticospinal pathways will not show use-dependent remodeling above the severe contusion injury and that ii) spared reticulospinal pathways will show use-dependent sprouting in segments below but not above the severe contusion injury.

Material & Methods

Animals and behavior training. All experimental procedures were previously used and described in details (van den Brand *et al.*, 2012; Beauparlant *et al.*, 2013). Experiments were conducted on adult female Lewis rats (200-220 g body weight) housed individually on a 12-hour light/dark cycle with access to food and water *ad libitum*. All experimental procedures were approved by the Veterinary Office of the Canton of Vaud. Prior to surgery, all the rats were first acclimatized to wearing the custom-made jacket for 1-2 weeks while navigating freely along the runway.

Surgical procedures. All surgical interventions were performed in aseptic conditions, under isoflurane full anesthesia (1-2%). All animals received postoperative analgesia and antibiotics for 3 and 5 days, respectively. Prior to spinal cord injury, all chronic SCI rats were implanted with electrodes: stimulating epidural electrodes (spinal segments L2 and S1) and recording EMG electrodes on flexor (tibialis anterior) and extensor (medial gastrocnemius) muscles of hindlimbs, bilaterally. The electrodes' wires were secured to the dura by stitches and arranged subcutaneously along the spinal cord to connect a headplug, which was plugged in during training sessions and functional evaluations.

Contusion injury. In our contusion model, SCI was the result of the impact of a weight dropped at T9 level and delivered by a force-controlled device (Infinite Horizon Impactor). The desired output was set to 250 kDyn (1 dyn = 10 μN). After a T9 laminectomy and exposure of the underneath dura, the weight was dropped directly on the dorsal aspect of the spinal cord and depth in tissue displacement was then measured by the device.

Experimental groups. In this study, we compared 4 different groups (**Figure 2**):

Healthy (n=4): Control animals which did not receive a SCI and were not trained.

Subacute (n=5): Control animals which received a SCI and were perfused in the subacute phase, i.e. 8 days post-SCI.

Non-trained (n=8): Control animals which received a SCI but were not trained.

Combo trained (n=8): Experimental group that received a neuroprosthetic rehabilitation training after a 1-week recovery post-SCI.
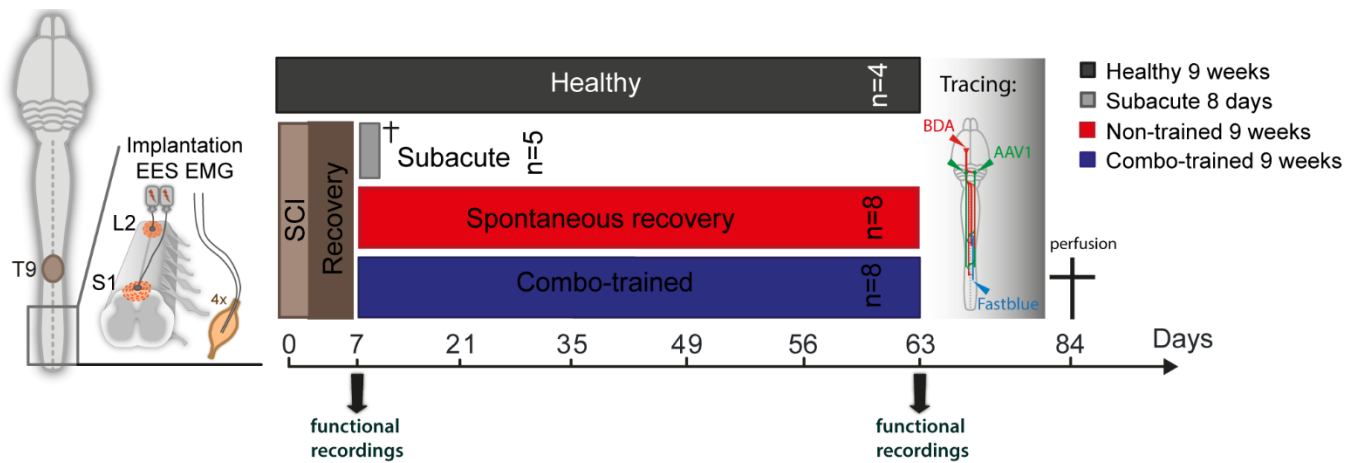
Figure 2. Timeline of the study protocol

Neuroprosthetic rehabilitation. Trained animals followed a rehabilitation program that was first described by van den Brand et al. (van den Brand *et al.*, 2012). Briefly, 10 minutes prior to training, rats received a systemic (i.p.) injection of a monoaminergic cocktail: serotonin receptor agonists 5-HT$_{1A/7}$ (8-OH-DPAT, 0.05-0.2 mg/kg) and 5-HT$_{2A/C}$ (quipazine, 0.2-0.3 mg/kg). This pharmacological stimulation was combined with electrical epidural stimulation (EES), delivered continuously during the training session (rectangular pulses of 0.2ms, 40Hz) through L2 and S1 implanted electrodes. Intensity of EES was adjusted (between 50-200μA) to obtain optimal facilitation of stepping visually. Active overground locomotion was promoted by the use of a home-made robotic postural interface (Dominici *et al.*, 2012) together with positive reinforcement. While this part of the training aimed at encouraging voluntary locomotion, we combined it with bipedal stepping on a treadmill (9 cm/s) with vertical robotic support to engage the denervated spinal circuits. The content of each training session evolved with the actual capacities of the rats and training objectives (van den Brand *et al.*, 2012). Rats were trained once per day in a single session of 25 minutes, 6 days per week.

Functional evaluation. One week (P7) and 9 weeks (P63) post-SCI, a set of recordings was performed in order to assess rats' performance under different paradigms. Tasks included walking over a flat surface, climbing stairs and swimming. All rats were recorded under the influence of the electrochemical neuroprosthesis. Recordings and data analysis of kinematics, kinetics and EMG have been described in previous studies (Musienko *et al.*, 2011; Courtine *et al.*, 2009; van den Brand *et al.*, 2012). The Vicon motion analysis system (Vicon Motion Systems, UK) was used to capture reflective markers attached bilaterally on the rat's iliac crest, hip, knee, ankle, metatarsophalangeal joint (MTP) and tip of the toe. EMG was recorded as well, through the implanted extensors and flexors electrodes.

Analysis was performed offline using the Nexus software (Vicon Motion Systems, UK) and custom-written Maltlab (MathWorks, USA) scripts.

Tracer injection. At the end of the training period (P63), rats were injected with tracers. To trace reticulospinal (ReST) fibers, an adeno-associated virus serotype 1 (AAV1) expressing GFP was injected bilaterally into the reticular formation (gigantocellular reticular nucleus). Three injections (300 nl per injection) were made bilaterally (Bregma -11, -11.5, -12mm) and 8 mm below the surface of the cerebellum. To trace motor cortex axonal projections originating from the left cortex, a 10% suspension of biotinylated dextran amine (BDA) was injected into the left motor cortex over 6 sites covering the hindlimb area (coordinates centered -1mm rostrocaudal and -1.75mm mediolateral to Bregma, depth 1.5mm). A third tracer, Fastblue (FB), was injected later (P74) at L2 level on the right side for a retrograde tract tracing of propriospinal neurons. However, its analysis was undertaken in another study.

Perfusion and tissue removal. In order to fix the tissue, at P84 (P8 or 10 for the sub-acute group), animals were perfused with a Ringer's solution containing 100 000 IU/L heparin and 0.25% $NaNO_2$ followed by 4% paraformaldehyde (PFA) in 0.1M phosphate buffer (PB), pH 7.4 containing 5% sucrose. Then the central nervous system composed of brain, brainstem and spinal cord was dissected, retrieved and post-fixed in PFA. Tissue was then transferred to 30% sucrose in PB for 5 days to attract water out of the cells before freezing. It was cut into blocks of defined spinal segments which were embedded individually in TissueTek O.C.T. (Sakura), frozen in -40°C isopentane and stored at -80°C until processing. For instance, segment C corresponds to T7-T8 levels, segment D contains the lesion and segment E contains T12-T13 levels.

Tissue processing, immunohistochemistry. Segments were cut into 40 µm thick coronal sections with a Leica CM 1950 cryostat. They were stored free-floating in 96-well plates filled with 0.1M phosphate buffered saline solution (PBS) or PBS azide. For each segment, we stained a sample consisting of sections spaced by approximately 960 µm. C segments were stained for GFP and BDA, while E segments were stained for GFP only.

Having injected AAV1 expressing GFP, the descending ReST fibers already expressed GFP, but with low signal. To enhance this signal, we stained the spinal cord slices by targeting the GFP molecule. Sections were washed in 0.1M PBS, incubated in a blocking solution (10% NGS, 1% Triton in PBS), incubated in serum containing primary antibody chicken anti-GFP (1:500 in 5% NGS, 1% Triton in PBS), washed again and revealed by a secondary antibody goat anti-chicken labelled with Alexa 488 (1:200 in 5% NGS, 1% Triton in PBS). BDA-labelled fibers were detected using streptavidin-horseradish peroxidase (1:200) in

0.1M PBS-Triton (1%), followed by amplification of the signal by Tyramine System Amplification (TSA) Cyanine 5 (PerkinElmer kit). The sections were left for drying before coverslipping with Mowiol.

In order to enable lesion reconstruction, segments D were stained for glial fibrillary acid protein (GFAP), a marker of astrocyte inflammatory response, and neuronal nuclei (NeuN), which is a specific marker of neuronal cell bodies. For GFAP, sections were blocked in 10% NGS, 1% Triton solution before being incubated overnight at 4°C in a 5% NGS, 1% Triton, rabbit anti-GFP antibody (1:1000, Dako, USA). They were incubated 60 minutes at room temperature in a 10% NGS, 1% Triton, goat anti-rabbit Alexa 488 (1:400, Invitrogen, USA) solution. For NeuN staining, sections were blocked for 2 hours at room temperature in 5% NGS, 0.4% Triton solution. Next, sections were incubated in a 2% NGS, 0.4% Triton, mouse anti-NeuN (1:500, Chemicon, USA) overnight at 4°C. The next morning, spinal cord sections were incubated 4 hours at 4°C in a 2% NGS, 0.4% Triton, anti-mouse antibody (1:500, Molecular Probes, USA) solution. Sections were mounted on slides, covered with Mowiol and coverslipped.

Neuromorphological evaluation. Confocal scans were acquired using a Leica TCS SPE microscope with a 20X objective and the LAS AF interface (Leica Microsystems, Germany). Three sections per animal and per segment were scanned, each consisting in 10 stacked images spread over an approximate depth of 20 µm and with an initial pixel size in the projection plane of 633nm x 633nm. Maximum intensity projection was computed to generate an output image of 8-bits with a decreased resolution of 400 pixels per mm of physical length. With the help of a custom-written Matlab script (van den Brand et al., 2012), we quantified fiber densities within selected regions of interest (ROI). Images were first color-filtered and the ROI drawn manually. They were binarized according to an intensity threshold that was kept constant across all animals. Density was computed as the ratio of positive pixels divided by the ROI area. Heat maps were also generated by the script.

Statistical analysis. Comparison between groups was assessed by a one-way ANOVA and when appropriate Fisher LSD test was applied (Prism, GraphPad Software, USA). All data are reported as mean values ± standard error of the mean (s.e.m.). A p-value < 0.05 was considered significant (*). P-value < 0.01 was marked (**) and p-value < 0.001 was marked (***). When not otherwise indicated on bar graphs, statistical symbols refer to unpaired t-test with the intact group.

Lesion reconstruction. Lesions were reconstructed using the Neurolucida software (Neurolucida, MBF Bioscience, USA). The spanning distance of a reconstruction along the spinal cord was 10.28mm, with a resolution of 320 µm between consecutive sections. Within each section analyzed, we traced by hand borders of the lesion delimited by GFAP staining. NeuN staining was used to trace borders of spared grey matter and of the section outline. Neurolucida provided a visual 3D-reconstruction of the spinal cord and lesion together with a 3D-morphological characterization of the lesion.

Results

Lesion reconstruction. We reconstructed the lesions of all animals with chronic SCI (**Figure 3** A). Lesion reconstruction for subacute animals was not considered, due to the overwhelming inflammatory response which would have biased the actual lesion contour. We found that lesions were highly variable in their shapes (**Figure 3** D), with a rim of spared white matter running along the ventral and lateral spinal cord.

The epicenter of a lesion was defined by its section having the smallest spared area. Initially expressed in absolute values (mm^2), spared areas were alternatively expressed as the ratio of spared area divided by the corresponding section area in a healthy animal, converted in percent. Since epicenter acts as a "bottleneck" for descending fibers, a relevant measure to characterize a lesion is its spared area at epicenter. Unexpectedly, we found that three months after injury, trained animals had a significantly larger fraction of spared area at epicenter ($p = 0.008$), although the initial lesion outcome, in terms of spinal cord displacement at time of impaction, was similar between the two groups ($p > 0.05$; **Figure 3** B).
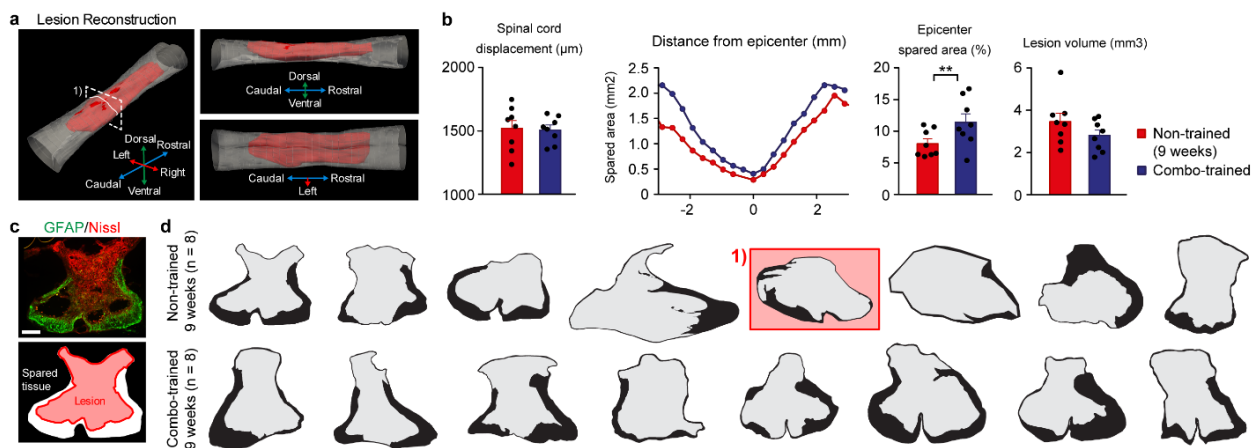

Figure 3. Variability of spared white matter after severe contusion SCI in trained and non-trained rats. A) 3D reconstruction of a contusion injury (highlighted within square in D). B) Comparison of the lesions' characteristics between trained and non-trained groups: spinal cord displacement at time of impaction and measures based on histological sections of the lesion. Error bars, s.e.m. C) Epifluorescent image showing an example of injury epicenter and its corresponding 2D contour tracing. Scale bar, 500µm. D) 2D contour tracing of injury epicenters of non-trained and combo-trained SCI animals.

Corticospinal pathway analysis. We visualized projections from the left hindlimb motor cortex by injection of biotinylated dextran amine (BDA). At the spinal level, corticospinal tract (CST) components are specifically labelled. The main tract is well-defined. In rodents, fibers descend in the contralateral dorsal column and project mainly to the dorsal horn with a small proportion entering the grey matter to re-cross the midline (**Figure 4**, inset). Since the contusion injury completely disrupts the corticospinal main tract, we confirmed histologically that there was no innervating fiber left from this tract below the lesion. Thus, we focused our analysis on the segment above the lesion.
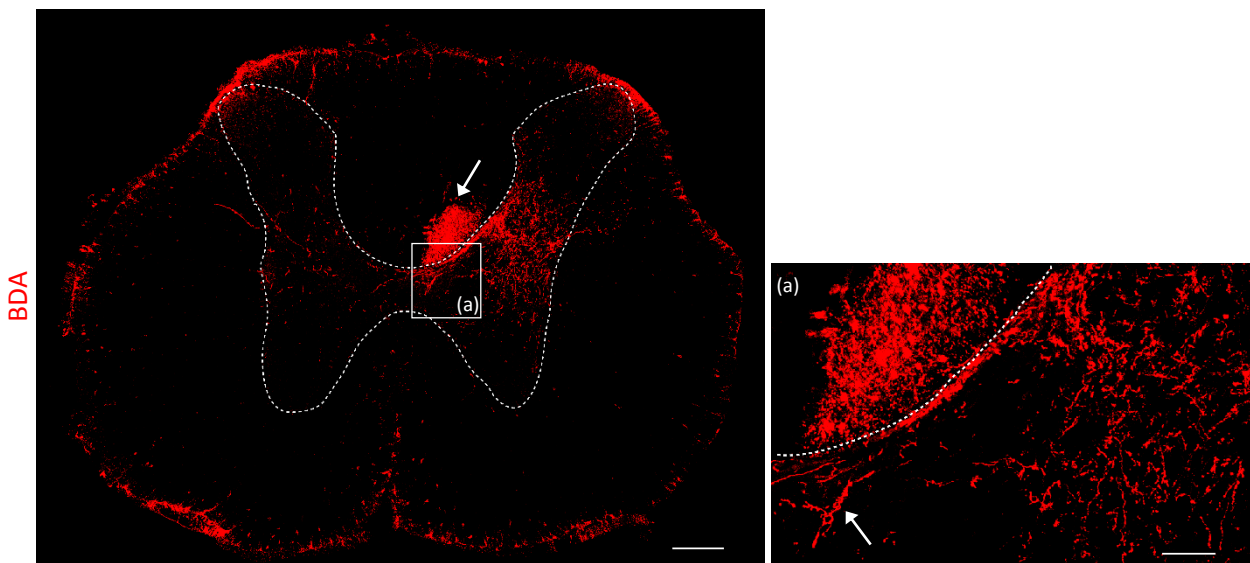

Figure 4. BDA-labeled CST in a healthy rat at thoracic level. Confocal image of labeled projections from the left hindlimb motorcortex showing the right corticospinal main tract (arrow) and its branching into the right grey matter. Inset: right corticospinal main tract projecting into the right grey matter and fibers recrossing the midline (arrow). Dashed line: grey matter contour. Scale bar, 200 µm; inset 50 µm.

We first measured fiber density in the right grey matter and found a significant increase in the chronic SCI non-trained group compared to both intact and subacute animals ($p < 0.05$). The chronic SCI trained group had a similar trend although not significant ($p = 0.17$; **Figure 5** A). A dorsoventral distribution of fiber density revealed that the site of this remodeling was the intermediate grey matter (**Figure 5** C).

Considering the critical localization of the corticospinal descending tract, we then assessed whether it was affected by the lesion in the segment above. Indeed, we found that CST white matter was significantly depleted in chronic SCI groups compared to the intact group ($p < 0.01$; **Figure 5** A). Interestingly, subacute animals also had less white matter spared compared to intact animals, but to

a lesser extent (p < 0.05), suggesting a time-dependent process in white matter withdrawal (**Figure 5** A, C).

Hence, it became relevant to normalize our previous grey matter raw data to the CST white matter. In this context, normalized fiber density corresponds to the fraction of innervating CST fibers branching from the descending tract to enter the grey matter at a given section level. It provides correction for the tracing procedure, for inter-individual variations in CST fiber number and for any injury-related axonal degradation. We found that right grey matter normalized fiber density was markedly increased in chronic SCI groups, compared to both intact (p < 0.01) and subacute (p < 0.05) groups. With left grey matter, we also found a significant increased density in chronic SCI groups compared to intact animals (p < 0.05; **Figure 5** B).
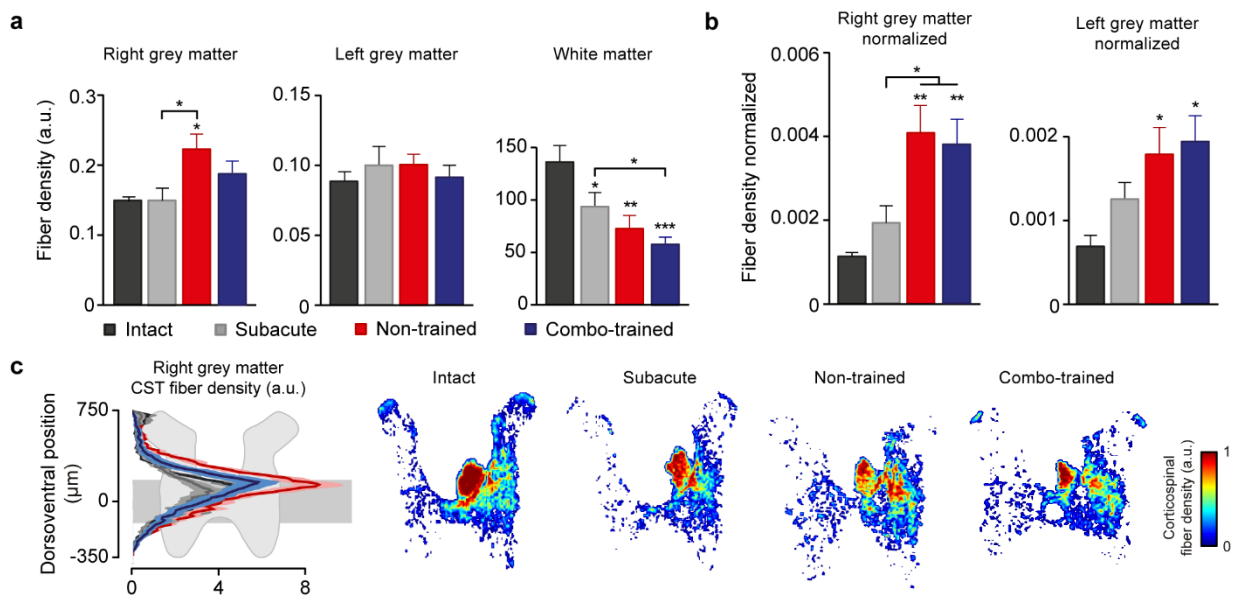

Figure 5. Severed CST is associated with spontaneous remodeling above the lesion. CST BDA-labeled fiber density analysis at T7/T8 level. A) Bar graphs reporting for each group fiber density within regions of interest: right and left grey matter and white matter. B) Normalized data for right and left grey matter. C) Dorsoventral density plot of fiber density in the right grey matter for each group and representative heatmaps of BDA-labeled fibers. *, p < 0.05; **, p < 0.01; ***, p < 0.001. Error bars, s.e.m.

Reticulospinal pathway analysis. We visualized the bilateral projections of the gigantocellular reticular formation by injection of an adeno-associated virus serotype 1 (AAV1) expressing green fluorescent protein (GFP) under the cytomegalovirus (CMV) promoter (AAV1-CMV-GFP). These projections belong essentially to the reticulospinal tract (ReST). In rodents, the ReST descends diffusely in the ipsilateral ventral, ventrolateral and lateral funiculi and innervates predominantly the grey matter ventral horns (**Figure 6**). When compared with the topography of the contusion lesion (**Figure 3**), one can observe that this tract is partially spared by the lesion. Thus, it can be considered as a potential substrate to mediate voluntary locomotion recovery. To assess this question, we analyzed ReST fibers above and below the lesion.
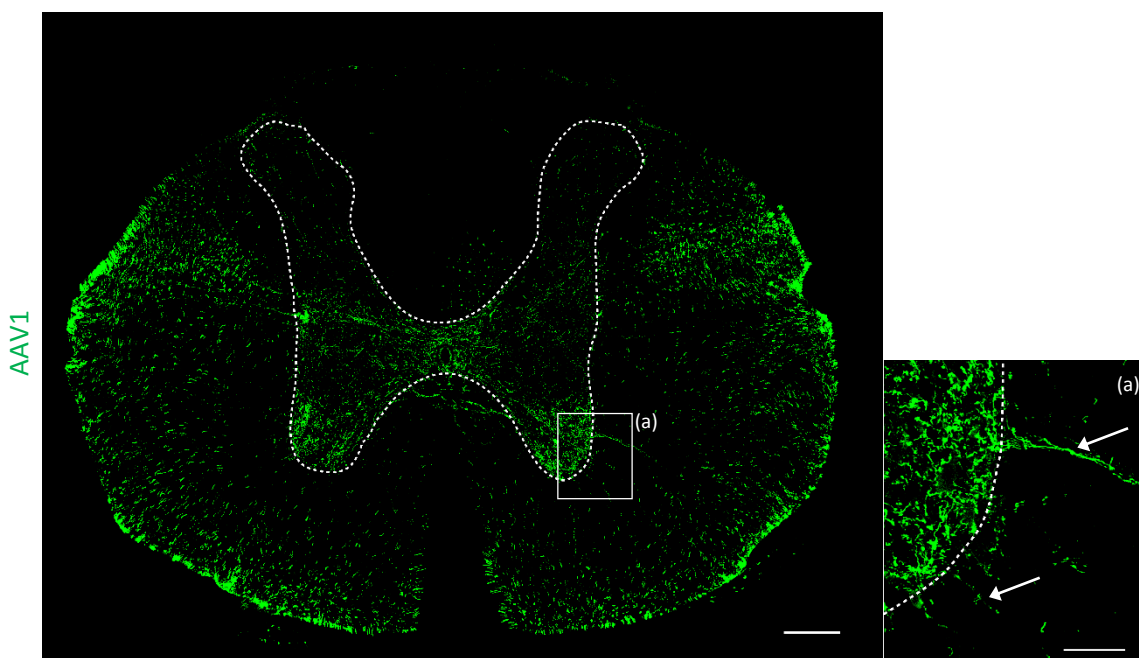

Figure 6. AAV1-labelled ReST in a healthy rat at thoracic level. Confocal image of labeled projections from the bilateral gigantocellular reticular formation. Inset: branching of ReST fibers into the ventral horn (arrows). Dashed line: grey matter contour. Scale bar, 200 µm; inset, 50 µm.

Above the lesion, we did not find a significant change in AAV1 fiber density between groups for the overall grey matter (**Figure 7** A). Similar to the corticospinal analysis, we normalized these data to fiber density of ReST in white matter. Since this normalization did not induce any change in the result, we continued the analysis without normalization.

Based on the ReST dorsoventral distribution, we next refined our analysis by dividing the overall grey matter in three areas: dorsal horns (laminae 1 to 6), intermediate grey matter (laminea 7 and 10) and ventral horns (laminae 8 and 9). None of these analyses revealed any significant difference between groups (**Figure 7** B). However, there was an overall trend towards intact animals having less fibers.
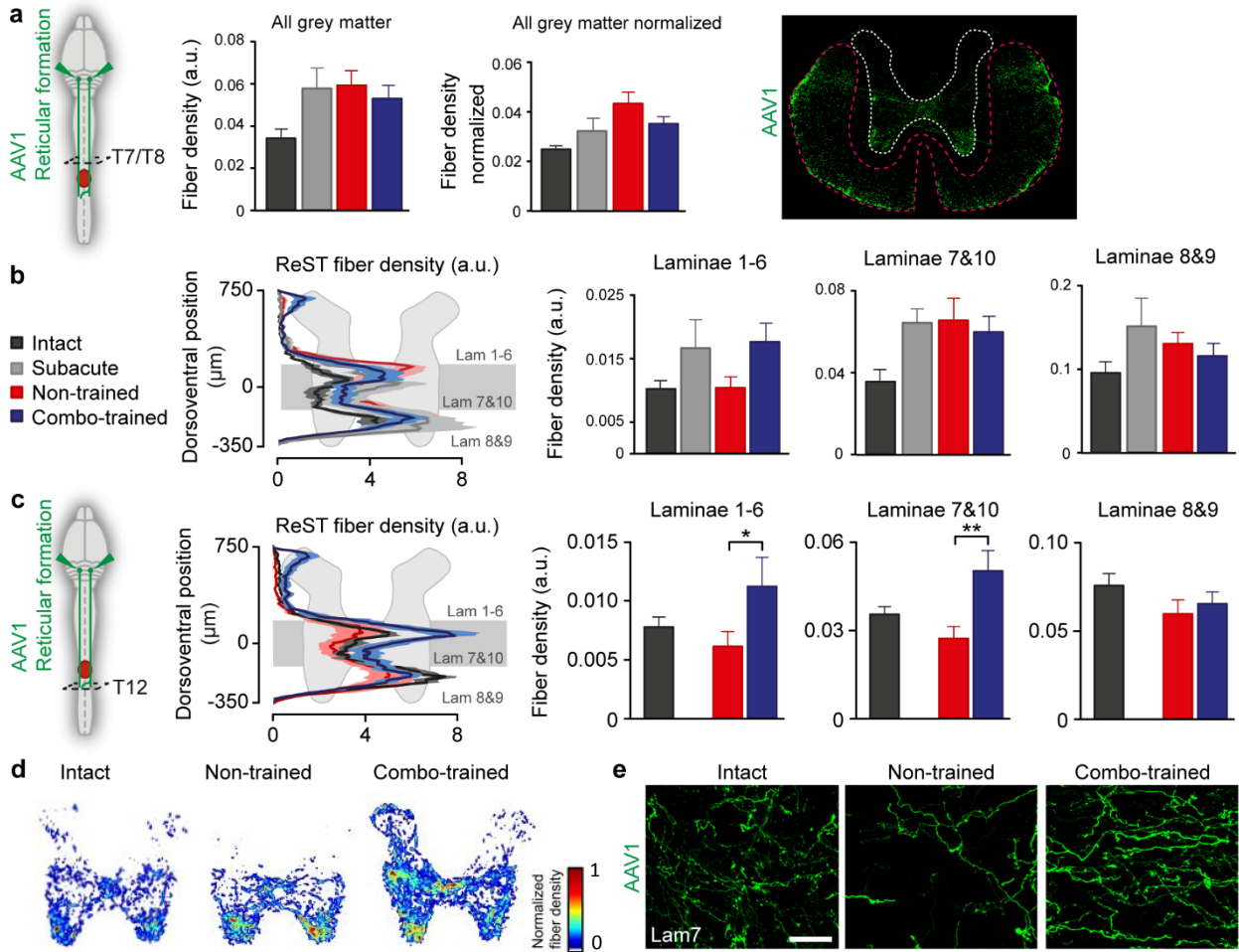

Figure 7. **Neuroprosthetic rehabilitation is associated with AAV1-labeled ReST remodeling below, but not above a severe contusion SCI.** A) Diagram illustrating anatomical experiment and bar graphs reporting the overall grey matter fiber density for each group, without normalization and normalized by white matter density. *Right.* Contour tracing of the ReST white matter region (pink dashed line) and grey matter region (white dashed line). B) Dorsoventral density plot and bar graphs reporting lamina-specific fiber density for each group. C) Diagram illustrating anatomical experiment. Dorsoventral density plot and bar graphs reporting lamina-specific fiber density for intact, non-trained and combo-trained groups. D) Representative heatmaps of AAV1-labeled reticulospinal fibers at T12/T13. E) Representative images of AAV1-labeled fiber density in lamina 7. Scale bar, 25μm. *, p < 0.05; **, p < 0.01. Error bars, s.e.m. Lam, lamina.

Below the lesion, trained animals showed an increased ReST fiber density in both dorsal (laminae 1 to 6) and intermediate (lamina 7 and 10) grey matter areas compared to non-trained rats (p < 0.05; **Figure 7** C), which surpassed intact innervation levels in some animals (**Figure 7** D, E). Reticulospinal axonal reorganization was primarily directed towards the intermediate laminae that are responsible for sensorimotor processing, while the motor-associated laminae 8 and 9 remained unaffected at T12/T13 (p= 0.77; **Figure 7** D, E).

Subacute data were not valid due to the tracing procedure. Indeed, in this group interference between the injury and migration of the AAV1 tracer can occur since these two events have to take place in a critically small time window in order to evaluate acute lesion effects.

Discussion

In this project, we have explored neural pathways reorganization underlying the recovery of voluntary movements in paralyzed rats with a severe contusion SCI. We have shown that spared reticulospinal axons reorganize with neuroprosthetic rehabilitation to reinforce connectivity with the segment below the lesion mainly by strengthening innervation of the intermediate spinal laminae.

We demonstrated the absence of use-dependent sprouting of the CST above the lesion but that, instead, CST sprouting occurs spontaneously at this level. This is consistent with the spontaneous CST sprouting reported in a dorsal hemisection at thoracic level with bilateral interruption of CST in rats (Bareyre *et al*. 2004). Our finding is closely related to what was found at the brainstem level using the same experimental groups, that is, a spontaneous increase in corticoreticular projections (**Figure 8**). Together, these results suggest that in response to lesioned spinal axonal projections, a process is activated rostral to the injury that generates an increased number of collaterals originating from the corticospinal pathway.
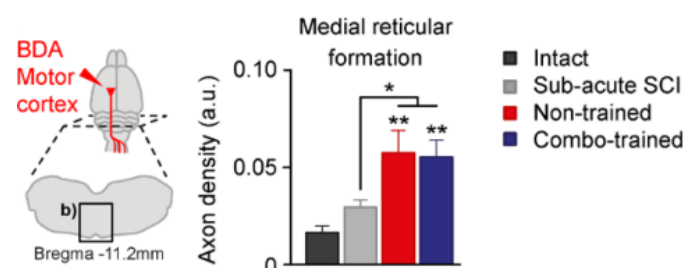

Figure 8. Spontaneous remodeling of motor cortex projections occurs in the presence of spared descending brainstem tracts. Diagram illustrating anatomical experiment and bar graph reporting the overall cortical axon density for each group. *Courtesy of Beauparlant J.*

We do not have a complete view of which are the targets of these collaterals, but in the absence of active training, we observe that it is not sufficient to mediate functional recovery in the case of a severe contusion SCI. Previous studies have emphasized on the role played by propriospinal neurons in reconnecting supraspinal inputs with efferent circuits, either spontaneously (Courtine *et al.*, 2008; Bareyre *et al.*, 2004) or following active training (van den Brand *et al.*, 2012). However, from a previous analysis performed in this laboratory, we know that in our model, there is no Fastblue (FB) retrograde labelling across the injury level, indicating that no propriospinal axon is spared at the lesion level (unpublished). Similar observation has previously been reported in both mild and severe contusion SCI (Conta & Stelzner, 2004). In contrast, we suggest here that spared ReST fibers can benefit from the spontaneous sprouting of CST above the lesion, in particular in the brainstem (**Figure 8**), but potentially also in thoracic segments (**Figure 9**), as they undergo remodeling through neuroprosthetic rehabilitation. In our clinically relevant SCI model, spared ReST fibers would thus play an essential pivotal role in restoring voluntary motor control over hindlimbs by re-establishing a signaling path between the hindlimb motorcortex and locomotor-related lumbosacral circuits (**Figure 9** C).
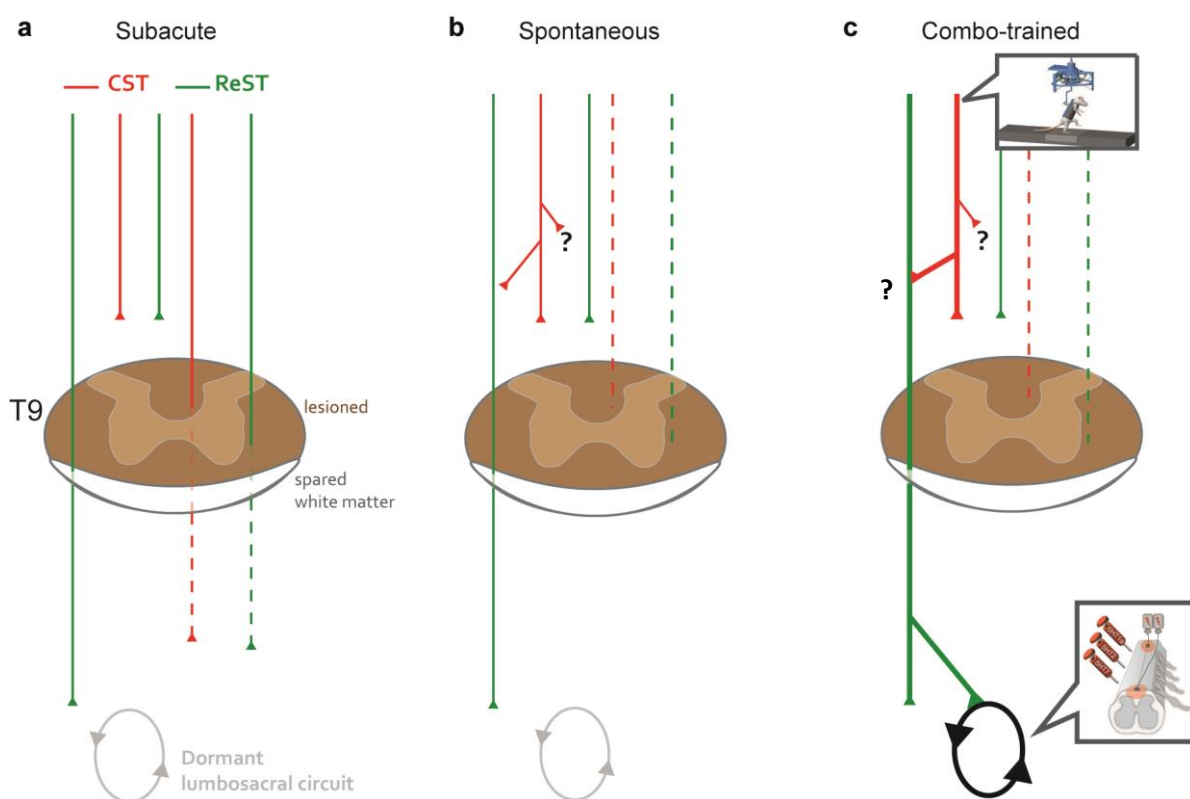

Figure 9. Model of ReST and CST reorganization following a severe but incomplete SCI in the rat. A) Subacute state. Dashed line, axonal degeneration. B) Spontaneous reorganization in the chronic phase (3 months post-SCI). Dashed line, axonal drawback. C) Reorganization in the presence of neuroprosthetic rehabilitation. Dashed line, axonal drawback.

Unlike cut injury models (for example: hemisection, transection, funiculotomy), only few anatomical studies have been conducted using contusion SCI. The underlying reason is that this model remains difficult to be systematized. Indeed, in this project, major issues were encountered inherent to the contusion lesion, which led to exclusion of some animals from the analysis.

First, there was a high variability in lesion size and morphology, as seen in the lesion reconstruction section. As a consequence, functional outcome was also varying within contused groups. Second, we found a surprisingly strong decrease in the amount of white matter CST fibers of the chronic SCI groups. Most likely, the explanation lies in axonal dieback (or "axonal drawback"). This phenomenon has been described following severed corticospinal axons in rats, although to a lesser degree: in a transection model, retraction bulbs of CST axons were visualized rostral to the lesion area at a distance that was not exceeding 3 mm 2 months post injury (Pallini *et al*., 1988). Using a model of moderate contusion SCI, another study found retraction bulbs as far as 5 mm rostral to the cavity 21 days post injury (Hill *et al*., 2001). In our case, we observed a massive decrease in descending CST fibers at an approximate distance of up to 5 to 6 mm away from the proximal lesion extremity. Together, these data suggest that the contusion induces a greater extension of axonal dieback than cut injuries.

Finally, we found that combo-trained animals had a significantly smaller lesion than non-trained animals. To our knowledge, such observation has never been reported for cut injury. We hypothesize that exercise-induced neuroprotection took place. A similar analysis of lesion size was conducted with rats trained in the same conditions but after a 3-months recovery (Helleboid PY, Master thesis 2013). No significant difference in lesion size was found between chronic trained and non-trained animals. This conclusion is consistent with our hypothesis, since neuroprotection, as a generalized process, takes place in the acute/subacute phase. A recent study further supports the concept of activity-induced neuroprotection (Jung *et al*., 2014): after six weeks of treadmill exercise in contused rats, increased expression of neurotrophic factors and suppression of apoptosis were measured in the spinal cord tissue.

Conclusion

During this project, we gained insight in the architectural rewiring underlying neuroprosthetic rehabilitation in a clinically relevant model of severe spinal cord injury. In contrast to previous cut injury model (van den Brand *et al.*, 2012), we found that a severe, yet incomplete, contusion SCI takes primarily advantage of spared reticulospinal axons to re-establish a supraspinal control over hindlimbs. Based on our results, we also highlighted the important role that secondary damages may play in a contusion injury. Complementarily targeting the microenvironment surrounding contused lesions might therefore optimize therapy based on a mechanistic approach.

Acknowledgments

References

Bareyre FM, Kerschensteiner M, Raineteau O, Mettenleiter T, Weinmann O, Schwab ME. The injured spinal cord spontaneously forms a new intraspinal circuit in adult rats. *Nat Neurosci* 2004; 7(3):269-77

Beauparlant J, van den Brand R, Barraud Q, Friedli L, Musienko P, Dietz V, Courtine G. Undirected compensatory plasticity contributes to neuronal dysfunction after severe spinal cord injury. *Brain* 2013; 136: 3347-61

Blesch A & Tuszynski MH. Spinal cord injury: plasticity, regeneration and the challenge of translational drug development. *Trends in Neurosci* 2008; 13(1):41-47

Bradbury EJ, Moon LD, Popat RJ, King VR, Bennett GS, Patel PN, Fawcett JW, McMahon SB. Chondroitinase ABC promotes functional recovery after spinal cord injury. *Nature* 2002; 416(6881):636-40

Brösamle C, Schwab ME. Cells of origin, course, and termination patterns of the ventral, uncrossed component of the mature rat corticospinal tract. *J. Comp. Neurol.* 1997; 386:293-303

Conta AC & Stelzner DJ. Differential vulnerability of propriospinal tract neurons to spinal cord contusion injury. *J. Comp. Neurol.* 2004; 479:347-359

Courtine G, Bunge MB, Fawcett JW, Grossman RG, Kaas JH, Lemon R, Maier I, Martin J, Nudo RJ, Ramon-Cueto A, Rouiller EM, Schnell L, Wannier T, Schwab ME, Edgerton VR. Can experiments in nonhuman primates expedite the translation of treatments for spinal cord injury in humans? *Nat Medicine* 2007; 13(5):561-66

Courtine G, Song B, Roy RR, Zhong H, Herrmann JE, Ao Y, Qi J, Edgerton VR, Sofroniew MV. Recovery of supraspinal control of stepping via indirect propriospinal relay connections after spinal cord injury. *Nat Medicine* 2008; 14(1):69-74

Courtine G, Gerasimenko Y, van den Brand R, Yew A, Musienko P, Zhong H, Song B, Ao Y, Ichiyama RM, Lavrov I, Roy RR, Sofroniew MV, Edgerton VR. Transformation of nonfunctional spinal circuits into functional states after the loss of brain input. *Nat Neurosci* 2009; 12(10):1333-42

Dimitrijevic MR, Faganel J, Lehmkuhl D, Sherwood A. Motor control in man after partial or complete spinal cord injury. *Advances in Neurology* 1983; 39: 915-26.

Dominici N, Keller U, Vallery H, Friedli L, van den Brand R, Starkey ML, Musienko P, Riener R, Courtine G. Versatile robotic interface to evaluate, enable and train locomotion and balance after neuromotor disorders. *Nat Medicine* 2012; online publication doi:10.1038/nm.2845

Helleboid PY. Reorganization of reticulospinal projecctions through multi-system neuroprosthetic training after severe chronic contusion spinal cord injury in rats. Master thesis 2013; EPFL

Hill CE, Beattie MS, Bresnahan JC. Degeneration and sprouting of identified descending supraspinal axons after contusive spinal cord injury in the rat. Experimental Neurology 2001; 171:153-69

Hollis ER & Zou Y. Expression of the Wnt signaling system in central nervous system axon guidance and regeneration. *Frontiers in Molecular Neuroscience* 2012; 5:1-4

Jung SY, Kim DY, Yune TY, Shin DH, Baek SB, Kim CJ. Treadmill exercise reduces spinal cord injury-induced apoptosis by activating the PI3K/Akt pathway in rats. *Experimental and Therapeutic Medicine* 2014; 7:587-593

Kakulas BA. A review of the neuropathology of human spinal cord injury with emphasis on special features. *The Journal of spinal Cord Medicine* 1999; 22:119-24

Lee BB, Cripps RA, Fitzharris M, Wing PC. The global map for traumatic spinal cord injury epidemiology: update 2011, global incidence rate. *Spinal Cord* 2014; 52(2):110-6

Metz GAS, Curt A, van de Meent H, Klusman I, Schwab ME, Dietz V. Validation of the weight-drop contusion model in rats: a comparative study of human spinal cord injury. *Journal of Neurotrauma* 2000; 17(1):1-17

Musienko P, van den Brand R, Maerzendorfer O, Larmagnac A, Courtine G. Combinatory electrical and pharmacological neuroprosthetic interfaces to regain motor function after spinal cord injury. *IEEE Transactions on biomedical engineering* 2009; 56(11):2707-11

Musienko P, van den Brand R, Märzendorfer O, Roy RR, Gerasimenko Y, Edgerton VR, Courtine G. Controlling specific locomotor behaviors through multidimensional monoaminergic modulation of spinal circuitries. *J. Neurosci* 2011; 31:9264-78

Norenberg MD, Smith J, Marcillo A. The pathology of human spinal cord injury: defining the problems. *J. Neurotrauma* 2004; 21:429-40

Pallini R, Fernandeez E, Sbriccoli A. Retrograde degeneration of corticospinal axons following transection of the spinal cord in rats. *J Neurosurg* 1988; 68:124-28

Schnell L, Schwab ME. Axonal regeneration in the rat spinal cord produced by an antibody against myelin-associated neurite growth inhibitors. *Nature* 1990; 343(6255):269-72

Tuszynski MH & Steward O. Concepts and methods for the study of axonal regeneration in the CNS. *Neuron* 2012; 74(5):777-91

Van den Berg MEL, Castellote JM, Mahillo-Fernandez I, de Pedro-Cuesta J. Incidence of spinal cord injury worldwide: a systematic review. *Neuroepidemiology* 2010; 34:184-92

Van den Brand R, Heutschi J, Barraud Q, DiGiovanna J, Bartholdi K, Huerlimann M, Friedli L, Vollenweider I, Moraud EM, Duis S, Dominici N, Micera S, Musienko P, Courtine G. Restoring voluntary control of locomotion after paralyzing spinal cord injury. *Science* 2012; 336(6085):1182-85